Near-infrared surface photometry of early-type spiral galaxies

II. M/L ratios and dark halos[*]

G. Moriondo[1], C. Giovanardi[2], and L.K. Hunt[3]

[1] Dipartimento di Astronomia e Scienza dello spazio, L.E. Fermi 5, I-50125 Firenze, Italy
[2] Osservatorio Astrofisico di Arcetri, L.E. Fermi 5, I-50125 Firenze, Italy
[3] C.A.I.S.M.I., L.E. Fermi 5, I-50125 Firenze, Italy

Abstract. We present mass distributions obtained from near-infrared (NIR) surface brightness decompositions and rotation curve fitting of a sample of early-type spiral galaxies. Bulge and disk mass-to-light (M/L) ratios, dark halo parameters, and the modified Newtonian dynamics (MOND) acceleration parameter are derived. We find that the mean disk NIR M/L is higher than that of the bulge, and comparison with stellar population synthesis models implies that early-type spiral bulges are, on average, younger and more metal rich than disks. NIR disk M/L is found to depend on disk luminosity, consistently with previously reported trends in ellipticals and spirals, and with cold dark matter models for disk formation. Within the optical radius, the mean ratio of stellar to dark matter is 2 and the typical dark halo mass is $10^{11}\,M_\odot$. The value of the MOND acceleration parameter that best accommodates the sample as a whole is $1.3 \cdot 10^{-8}\,\mathrm{cm\,s^{-2}}$.

Key words: galaxies: fundamental parameters – galaxies: kinematics and dynamics – galaxies: spiral – galaxies: stellar content – galaxies: structure

1. Introduction

The comparison of the luminosity profiles and rotation curves of disk galaxies provided the first evidence for dark matter in outer parts of galaxies (e.g., van Albada & Sancisi 1986). The luminous material, either in the form of stars or neutral gas, is not able to reproduce the approximate flatness of the rotation curves at large radii, implying that the Newtonian theory of gravitation needs to be modified or that the mass in the outer regions of most spirals is dominated by a dark component. The physical extent of such a "dark halo" cannot be inferred from the rotation curves, since these last are flat even where the luminous material ceases to be detected. Hence, the total mass in spiral galaxies is not yet well known.

The properties of dark matter (DM) and the structure of dark halos as derived from rotation curves have profound implications on cosmological issues such as galaxy formation. Recent N-body simulations of cold dark matter halos together with adiabatic infall models have shown that matching observed rotation curves requires a systematic increase of disk mass-to-light ratios with luminosity (Navarro et al. 1996). Such a trend is observed in large bodies of rotation curve data (Broeils 1992; Persic et al. 1996 – hereafter PSS), and further comparisons between theoretical predictions and observations may help clarify the nature of dark matter in galaxies.

The presence of a dark halo makes global mass-to-light (M/L) ratios derived from rotation curves much higher than those expected from stellar populations, and produces radial gradients in the total M/L. The contribution of DM tends to be larger for low-luminosity systems, as the fraction of DM to luminous matter within the optical radius appears to decrease with increasing galaxy luminosity (Kormendy 1990; Salucci et al. 1991). In luminous systems, therefore, the mass distribution in the inner few disk scale lengths can be largely ascribed to the bulge and disk stars. Consequently, when stellar galaxy components can be accurately isolated with surface photometry, estimates of their M/L from rotation curves provide useful constraints for the age, abundance, and star formation history of their stellar populations. Recent population synthesis models predict trends of M/L with metallicity and with wavelength (Worthey 1994; Bruzual & Charlot 1993), and can be used to infer and compare properties of the stellar populations in bulges and disks.

We have reported in a previous paper (Moriondo et al. 1997 – hereafter Paper I) the results of two-dimensional near-infrared (NIR) surface brightness decompositions for a sample of early-type spirals. NIR wavelengths, especially when combined with those in the optical, are a powerful diagnostic tool since they trace more accurately the stellar mass content and minimize the complications of extinction. In this paper, we apply the bulge+disk decomposition results to the analysis of the rotation curves for our sample. In Sect. 2 we derive the radial mass distributions and evaluate the contribution of the bulge, disk, and dark halo to the observed rotation curves; as an alternative

to dark matter halos, we also derive a value of the modified Newtonian dynamics critical acceleration parameter. The resulting NIR M/L ratios of the luminous components are analyzed in Sect. 3, and compared with those at optical wavelengths and with population synthesis models. Finally, we assess the importance of dark halos, and explore trends of M/L with luminosity in the context of the properties of the fundamental plane for gravitationally bound objects (e.g., Burstein et al. 1997).

2. Data analysis

2.1. Surface photometry and structural decomposition

The techniques used to reduce and analyze the photometric data are detailed in Paper I. Briefly, we decomposed the surface brightness distributions of each sample galaxy into the two components of bulge and disk. Two independent methods were used: a) a parametric fit assuming a generalized exponential bulge plus an exponential thin disk; and b) an iterative non-parametric (np) decomposition algorithm. We emphasize that both procedures decompose the entire two-dimensional brightness distribution, rather than the brightness profiles, and take into account the effects of seeing. The bulge is assumed to be an oblate rotation ellipsoid coaxial with the disk. In addition to the NIR images, r band brightness profiles and M/L ratios (Kent 1988) are available for ten galaxies of our sample.

2.2. Observed rotation curves

Rotation curves (RC's) exist for all the galaxies in our sample; the references for them are shown in Table 1, together with general information regarding the sample. More information about the sample objects (coordinates, etc.) can be found in Paper I. HI data are available for six objects; for the remainder, RC's were obtained from optical emission lines. We discarded absorption data since they are likely to yield a lower limit rather than a true estimate of the rotational velocity, due to the effect of velocity dispersion and projection along the line of sight. All distances were scaled to match our values, and circular speeds were corrected when estimated from inclinations differing from ours, with the exception of extended HI RC's derived from interferometric maps.

2.3. Model rotation curves

To determine the shape of the RC for our galaxies we assumed: a) optical transparency (which was also assumed for the surface brightness decompositions); and b) the M/L ratio of bulge and disk to be constant within each component. The circular velocity in the equatorial plane of an axisymmetric mass distribution is given by

$$v_c^2(r, 0) = r \left(\frac{\partial \Phi}{\partial r} \right)_{(z=0)} \tag{1}$$

where $\Phi(r)$ is the gravitational energy at radius r. In this case Φ is the sum of the contributions of bulge and disk and, when necessary, also of a dark halo.

Table 1. Galaxy sample and RC references.

Name	Distance [Mpc]	R_{25} [arcsec]	B_T [mag]	RC
(1)	(2)	(3)	(4)	(5)
NGC 1024	69.2	117	13.08	1
NGC 2639	70.4	55	12.56	1
NGC 2775	27.1	128	11.03	1
NGC 2841	19.2	244	10.09	2
NGC 3593	17.2	157	11.86	1,3,4,5
NGC 3898	34.8	131	11.60	1,6,7
NGC 4378	51.4	87	12.63	1
NGC 4419	23.9	99	12.08	1
NGC 4450	23.9	157	10.90	6,8
NGC 4698	23.9	119	11.46	1,5,9
NGC 4845	27.1	150	12.10	1
NGC 5879	26.2	125	12.22	6,10
NGC 6314	139.2	43	13.80	1
IC 724	125.6	70	13.40	1

Notes. Column 2: see paper I. *Columns 3-4*: values from the Third Reference Catalog of Bright Galaxies (de Vaucouleurs et al. 1991) *Column 5*: References for the RC's (O = optical, R = radio). 1: Rubin et al. 1985 (O); 2: Begeman 1987 (R); 3: Bertola et al. 1996 (O); 4: Demoulin 1969 (O); 5: Krumm & Salpeter 1979 (R); 6: Fillmore, Boroson & Dressler 1986 (O). For NGC 4450 we considered just the rising part of their observed curve, since the declining outer part is inconsistent with the 21 cm data from reference 8; 7: van Driel & van Woerden 1991 (R); 8: Guhathakurta et al. 1988 (R); 9: Warmels 1986 (R); 10: Broeils & van Woerden 1994 (R).

2.3.1. The bulge

The circular speed of an axisimmetric ellipsoidal distribution of matter is given by (Binney & Tremaine 1987):

$$v_c^2(r) = 4\pi G \, \Upsilon_b \, \sqrt{1 - \epsilon^2} \int_0^r \frac{j_b(a) a^2 \, da}{\sqrt{r^2 - a^2 \epsilon^2}} \quad, \tag{2}$$

where Υ_b is the bulge M/L ratio, $j_b(a)$ the luminosity density at distance a from the center in the equatorial plane, and $\epsilon = \sqrt{1 - b^2/a^2}$ the constant intrinsic eccentricity. To determine j_b from the brightness distribution, when $\epsilon \neq 0$ we cannot invert the Abel equation (e.g., Binney & Tremaine 1987) appropriate for spherical distributions. An alternative approach (see Appendix) considers the "strip brightness", $S(a)$, defined as the integral of the bulge brightness distribution along a path orthogonal to the line of nodes, at distance a from the center. Under the hypothesis of transparency, this quantity is independent of the inclination of the galaxy. Since

$$\frac{dS}{da} = -2\pi \sqrt{1 - \epsilon^2} \, a \, j_b(a) \tag{3}$$

it is straightforward to determine j_b (and hence the rotation speed from Eq. 2) once $S(a)$ has been evaluated from the brightness distribution. Eq. 3, in turn, can be expressed either in terms of a parametric or np profile respectively, depending on the kind of decomposition considered.

2.3.2. The disk

In the case of an infinitely thin exponential disk, the rotation speed is given by (Freeman 1970):

$$v_c^2(r) = 4\pi G \Sigma(0)\, r_D\, y^2 \left[I_0(y)K_0(y) - I_1(y)K_1(y) \right] \ , \quad (4)$$

where $y = r/(2r_d)$, I_n and K_n are the modified Bessel functions of first and second kind, respectively; $\Sigma(0) = \Upsilon_d\, I(0)$ is the central disk surface density, and r_d the disk scale length.

For the np disk we have adopted the following expression for the circular speed (Toomre 1963; Kent 1986):

$$v_c^2(r) = 2\pi r G \int_0^\infty a\, \Sigma(a)\, H(a,r)\, da \qquad (5)$$

where $\Sigma(a)$ is again the disk surface density, and

$$H(a,r) = \frac{2}{\pi a r} \left[K(k) - \frac{E(k)}{1-k^2} \right], \quad k = \frac{r}{a}, \ \text{for } r < a \quad (6)$$

$$= \frac{2\, E(k)}{\pi r^2 (1-k^2)}, \quad k = \frac{a}{r}, \ \text{for } r > a \quad (7)$$

Here $K(k)$ and $E(k)$ are the complete elliptic integrals of first and second kind, respectively. Equation 5 can be rewritten in the more condensed form

$$v_c^2(r) = 4G r \left\{ \int_0^1 \frac{t\, E(t)}{1-t^2} \Sigma(rt)\, dt \ + \right.$$
$$\left. + \int_0^1 \left[K(t) - \frac{E(t)}{1-t^2} \right] \Sigma \left(\frac{r}{t} \right) \frac{dt}{t^2} \right\} \qquad (8)$$

which we have used in our computations.

2.3.3. The dark halo

We have considered two different spherical distributions of matter to model the dark component. The first is a pseudo-isothermal sphere (Kent 1986) with density profile:

$$\rho(r) = \frac{v_h^2}{4\pi G(r^2 + r_h^2)} \qquad (9)$$

and circular speed:

$$v_c^2(r) = v_h^2 \left[1 - \left(\frac{r_h}{r} \right) \arctan \left(\frac{r}{r_h} \right) \right] \qquad (10)$$

where v_h, the asymptotic circular speed, and r_h, the scale length, are parameters of the distribution. The second is a sphere of constant density ρ_0, with

$$v_c^2(r) = \frac{4r^2}{3\pi G \rho_0} \qquad (11)$$

where ρ_0 is the only parameter of the distribution. This distribution, with v_c linearly increasing with r, is suited in some cases to represent the inner part of the halo RC; it is in fact the limit of Eq. 10 for $r \ll r_h$. We have adopted it whenever measurements of circular speed did not extend beyond the optical radius. In most cases the two models are mutually exclusive, since the latter cannot fit a flat RC, whereas v_h is not constrained if the data are restricted to the rising part of the RC.

2.4. Modified Newtonian dynamics

To test the predictions of modified Newtonian dynamics (MOND: Milgrom 1983; Sanders 1990; Begeman et al. 1988 – hereafter BBS), we have altered our model RC's according to the prescriptions given by BBS. In particular, the relation between Newtonian ($\mathbf{g_n}$) and modified ($\mathbf{g}$) acceleration

$$\mathbf{g_n} = \mathbf{g}\, \mu(\mathbf{g}/\mathbf{a_0})$$

with

$$\mu(x) = x(1+x^2)^{-1/2}$$

can be used to derive the modified expression for the circular velocity.

Although in most cases the available RC's are not very extended, in six cases (namely NGC 1024, NGC 2841, NGC 3593, NGC 4698, NGC 5879, and IC 724), the critical acceleration ($a_0 \sim 10^{-8}\,\mathrm{cm\,s^{-2}}$) is achieved within the radius sampled by the RC. These objects therefore can provide a test for MOND.

3. Results

3.1. Rotation curve fitting

With the exception of NGC 2841 and perhaps NGC 4698, our rotation curves do not extend far enough to constrain effectively both the stellar M/L's and the halo parameters of Eq. 10, and result in high uncertainties on the parameters (of order 50%) when all of them are fit simultaneously. Moreover, a global fit of the three components, at least in the case of the isothermal halos, tends to attribute most of the mass to the halo at all radii. These difficulties were also noted by Kent (1988), who considered further assumptions and simplifications to better constrain the parameter space. In particular he suggested three possible kinds of fits.

a) Maximum bulge+disk solutions (MBD hereafter), in which the maximum amount of mass compatible with the rotation observed is ascribed to the visible matter. This can be achieved by fitting the RC with only the two stellar components for radii within two disk scale lengths, or up to the disk velocity peak for the np case. When the observed RC is constant or rising beyond this limit the dark halo contribution is added. In our case the MBD approach can be justified by noting that these are all relatively high-luminosity objects with $L \sim L^*$, so that DM should not be important in the inner regions (Kormendy 1990; Salucci et al. 1991); in general the rising part of the RC is well reproduced, confirming that this hypothesis is probably correct. Moreover, in the case of NGC 2841 the simultaneous fit of the three components does not differ appreciably from the MBD one. For NGC 4698 it yields M/L ratios for disk and bulge lower by about a factor of two, although with higher uncertainties which make the result again consistent with the MBD results.

b) Fits with fixed asymptotic halo velocity, v_h. If we assume that this parameter can be determined from the flat portion of the RC, the number of free parameters is reduced to three. Only a few of our galaxies have extended RC's, so that an independent

estimate of v_h is possible only for NGC 2841 and NGC 4698. In these two cases, however, the fitting routine is able to estimate v_h with reasonable accuracy (the uncertainty is $< 15\%$), so that we did not consider this kind of solutions.

c) Fits with constant-density halos. Adopting the halo distribution described by Eq. 11, again we have only three free parameters. We find that in general such a halo does not affect appreciably the contribution of bulge and disk to the rising part of the RC, thus yielding M/L's consistent with the MBD values.

On the basis of the above statements, and to define a homogeneous set of parameters, we decided to consider only the MBD solutions, assuming that the associated errors are realistic estimates of the true parameter uncertainties. The dark halo contribution was added for six galaxies out of 14; five of these have RC's measured at 21 cm, while for the sixth, NGC 2639, the optical RC was sufficient to constrain the halo contribution. In the case of NGC 3593, the radio measurements, extending to about 1.5 R_{25}, could be fit reasonably well without any dark component. For each galaxy we chose the model halo (the constant density or the pseudo-isothermal sphere) which yielded the best-quality RC fit; the constant-density halo was adopted for NGC 2639, NGC 4450, and NGC 5879. Comparing quantities which can be derived in both cases, such as the central density or the mass within the optical radius, we find no systematic difference between the two models.

The resulting M/L's and halo parameters are given in Table 2, and Table 3 reports the masses of the various components. The values presented in the tables are the mean of the parametric and np results; the error is the largest of the values for the semi-difference (parametric and np) and the formal error on the fitted parameter. Fig. 1 illustrates the fits to the observed rotation curves for both the parametric and np surface brightness decompositions. We note that the best results in most cases are obtained with the np fits, which in general match more closely the features of the observed curves. Quantitatively, comparing the χ^2 obtained in the two cases, we find a median ratio of the parametric to the np value of 1.3.

3.2. M/L ratios

Disks have a mean M/L ratio of 1.6 and 1.0 (solar units) in J and K, with a dispersion of 0.6 and 0.4, respectively; the mean bulge M/L is 1.1 ± 0.6 in J and 0.6 ± 0.2 in K. We note that five galaxies (namely NGC 2639, NGC 3593, NGC 3898, NGC 4419 and NGC 5879) yield low values of bulge M/L; these were excluded from the mean calculation (see Sect. 4.1). For NGC 4698, this happens only in the np case. Note that NGC 3593 and NGC 4419 are actively forming stars (Paper I), so a low M/L might be expected. Kent (1988) also found low M/L ratios for these five galaxies, and interpreted this as an inconsistency between photometric and kinematical data, possibly due to non-circular motions of the ionized gas in the inner part of the galaxies. The same conclusion was attained by Fillmore et al. (1986), who have modeled both rotation and velocity dispersions from emission and absorption-line data for six galaxies, three of which are also in our sample (see Table 1). Their models suggest that in most

cases even the observed emission-line velocity underestimates the actual RC of the galaxy in the inner regions ($r < 1$ kpc). In the case of NGC 3898 and NGC 4450, for instance, a rough estimate of the bulge M/L from their model RC turns out to be respectively six and two times higher than ours. Even these 'corrected' values, however, remain lower by at least 15% than the disk M/L's estimated from the observed rotation.

3.3. Dark halos

The dark halo parameters we obtain are similar to the ones derived for other samples, in particular for later type spirals using photometry in the optical passbands (e.g., Kent 1986; Kent 1987). Scale lengths r_h are comparable to the optical size of the galaxies and range from 18 to 30 kpc; the average halo mass is about 10^{11} M$_\odot$ within R_{25}. The central halo densities show a rather narrow distribution, peaked at $30 \cdot 10^{-26}$ g cm^{-3}, with a dispersion of about 20%. The average ratio of luminous to dark matter within the optical radius is around 2, a typical value for bright spirals (PSS).

3.4. MOND

For the six objects selected in Sect. 2.4, we first performed a fit of the RC with a_0 and the bulge and disk M/L as free parameters. This yielded for a_0 a weighted mean of 1.3 in units of 10^{-8} cm s^{-2}. We then performed two sets of fits keeping a_0 fixed respectively to our value of 1.3 and to the value of 0.8, corresponding to the $a_0 = 1.21$ obtained by BBS rescaled to $H_0 = 50$ km s^{-1}.

A visual inspection of the observed RC's and the models does not clearly favor one paradigm over the other. This qualitatitve statement is confirmed by the similar values of χ^2. Two representative cases are shown in Fig. 2: NGC 2841, for which MOND yields a particularly good fit, and NGC 5879 for which a dark halo seems to produce a significantly better result. The choice of a_0 turns out to be crucial only for NGC 2841, where only $a_0 = 1.3$ yields a good fit. BBS also found that this galaxy required a higher critical acceleration, probably because of an error in the estimated distance, and did not include it in their average. After removing NGC 2841 from the sample, the remaining five galaxies yield $a_0 = 0.74$, fully consistent with the BBS value.

4. Discussion

4.1. Stellar content

We have compared colors and M/L's for our sample with models of stellar population synthesis (SPS) to place constraints on age and metallicity of the average stellar content of bulges and disks. In particular we have considered Worthey's model (1994, W94 hereafter) for single stellar populations with ages from 1.5 to 17 Gyr and different metallicities, and the 1995 release of the model by Bruzual and Charlot (1993, BC95) for populations with solar metallicity and different star formation histories.
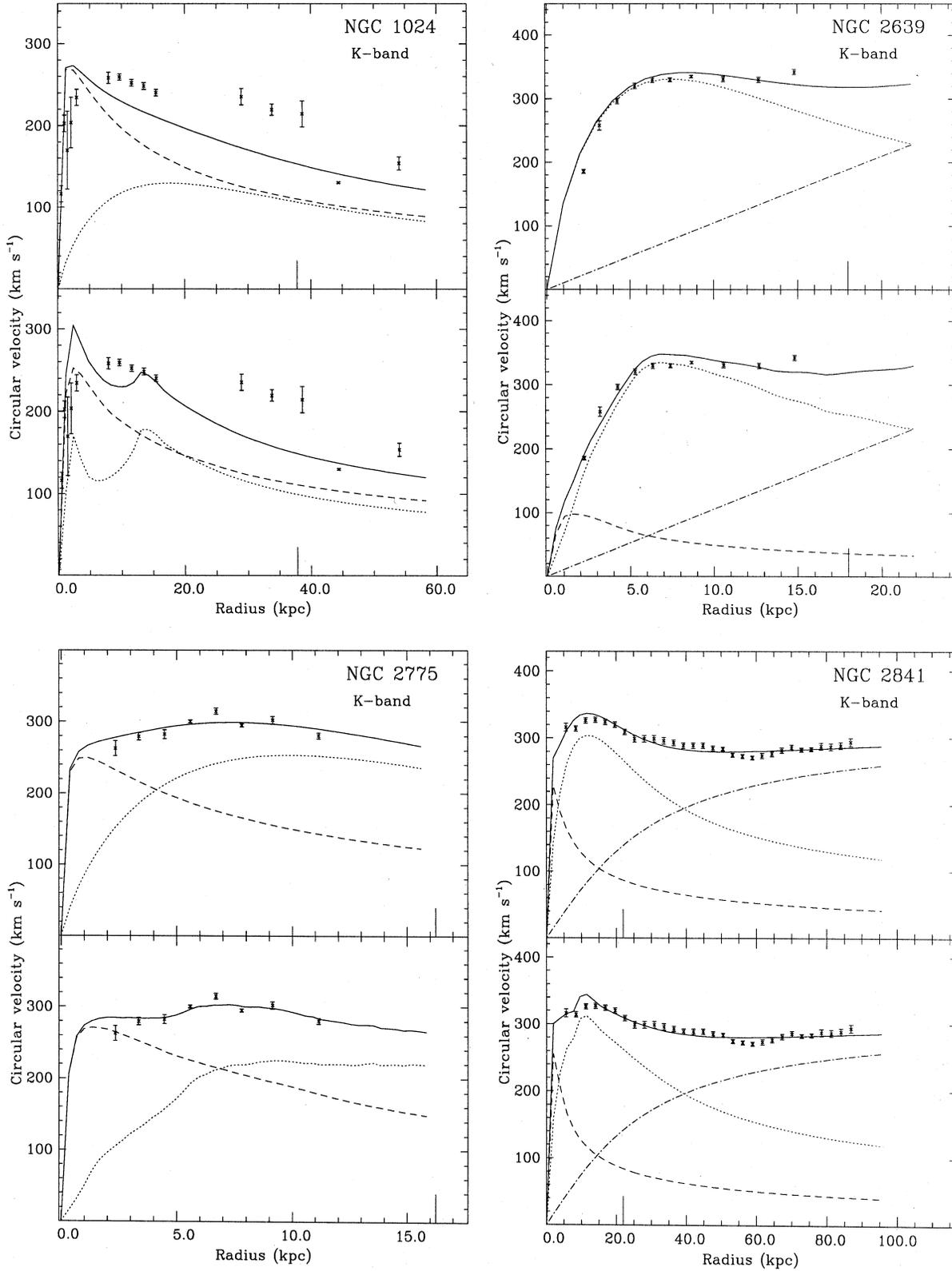
Fig. 1. Observed and fitted rotation curves. Upper and lower panels show respectively the results from parametric and np decompositions (K band). The dots are the observed curve; the dashed, dotted, and dot-dashed lines are respectively the contributions of bulge, disk, and dark halo to the model RC (continuous line). The mark on the abscissa corresponds to R_{25}.
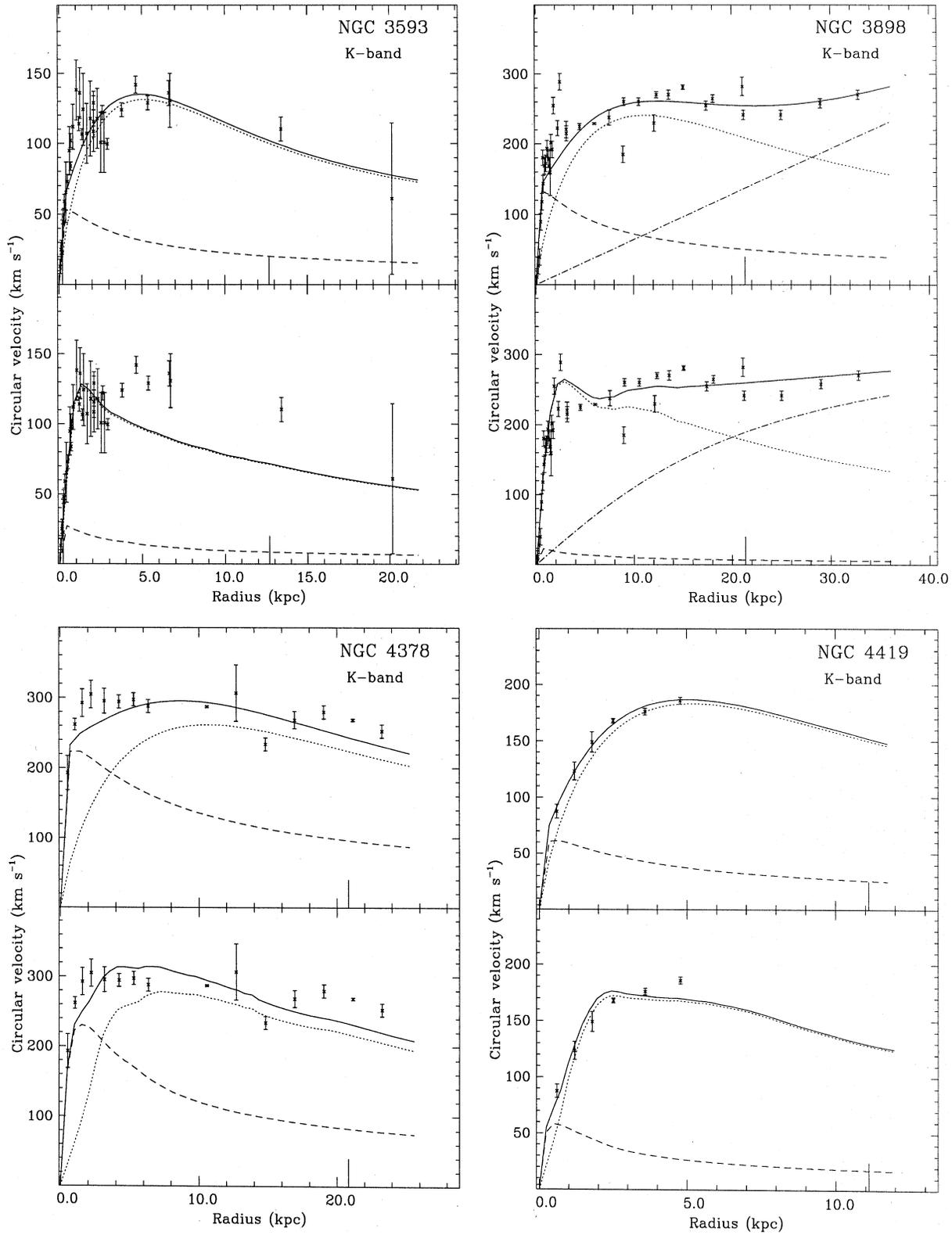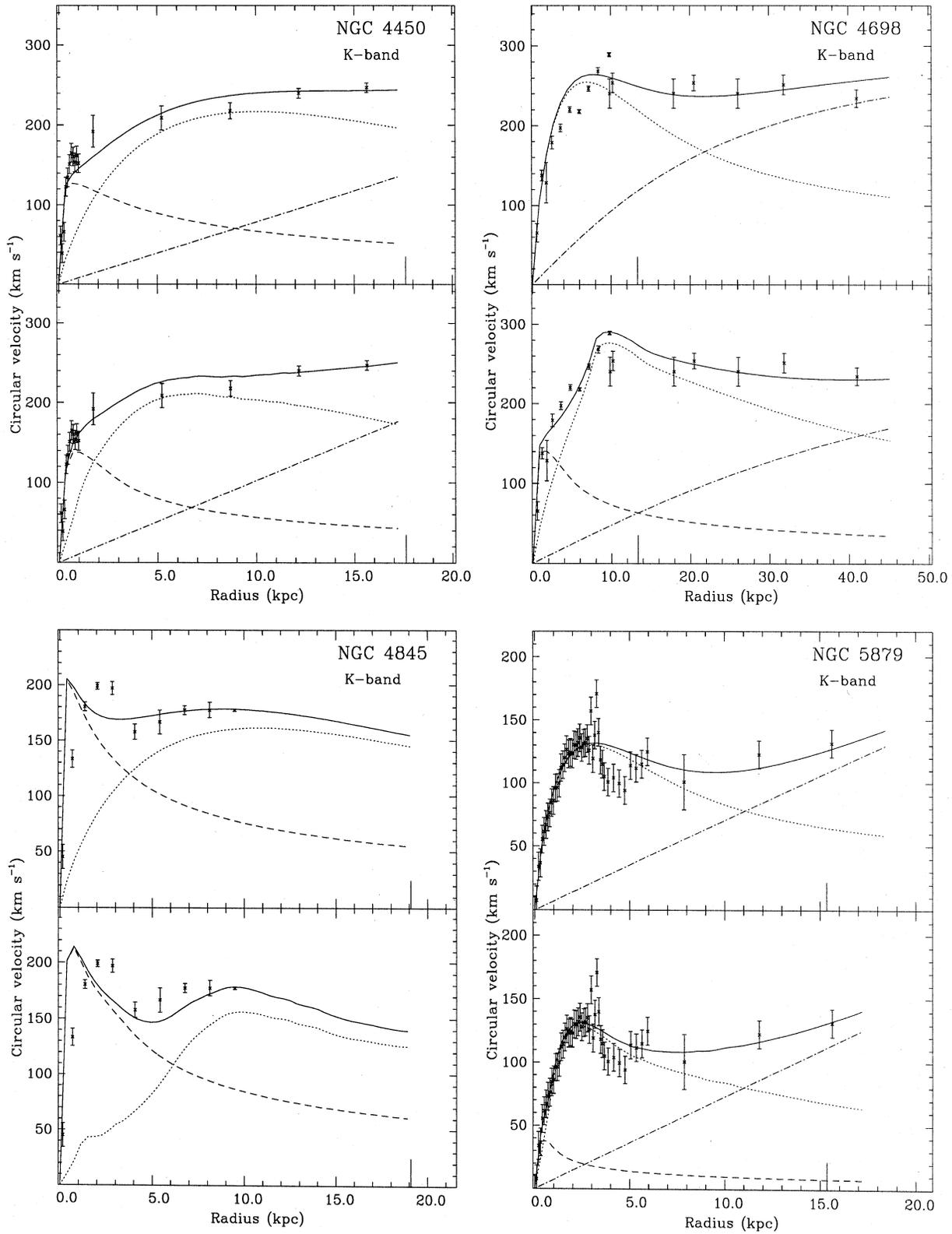
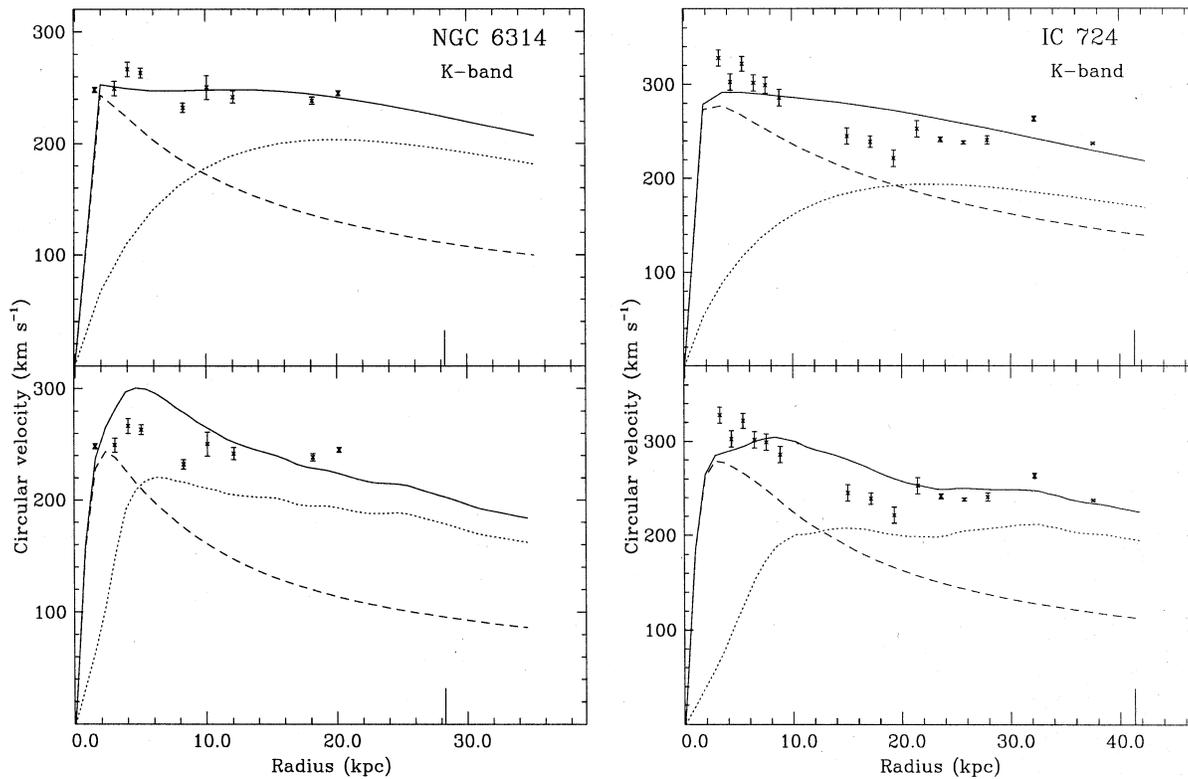**Fig. 1.** (continued)

Fig. 1. (continued)
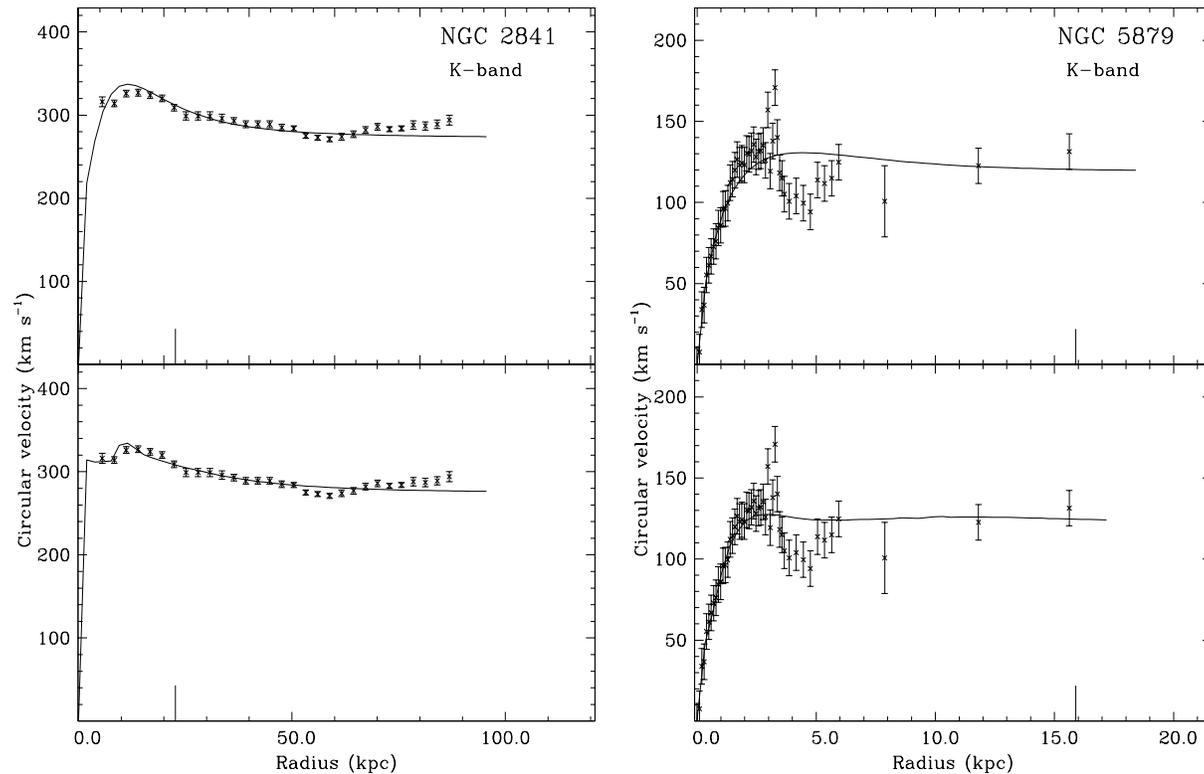
Fig. 1. (continued)

Fig. 2. Fit with MOND to the RC's of NGC 2841 and NGC 5879 from parametric (*upper panels*) and np decompositions (*lower panels*). Dots represent the observed RC, whereas the continuous line is the model one. In both cases we plot the results for $a_0 = 1.3$.

Table 2. Fits to the rotation curves: mass-to-light ratios and halo parameters.

Name	$(M/L_J)_b$	$(M/L_J)_d$	$(M/L_K)_b$	$(M/L_K)_d$	ρ_0 $[10^{-26} \text{g cm}^{-3}]$	r_h [kpc]	v_h [km s^{-1}]
(1)	(2)	(3)	(4)	(5)	(6)	(7)	(8)
NGC 1024	–	–	0.81 (0.20)	0.99 (0.48)	–	–	–
NGC 2639	0.00 (0.05)	1.79 (0.45)	0.06 (0.06)	1.03 (0.26)	41.6 (4.1)	–	–
NGC 2775	1.39 (0.20)	1.51 (0.15)	0.80 (0.10)	0.86 (0.08)	–	–	–
NGC 2841	1.70 (0.01)	2.39 (0.26)	0.90 (0.05)	1.25 (0.15)	22.1 (1.9)	23.7 (3.0)	315 (10)
NGC 3593	0.15 (0.04)	0.96 (0.36)	0.06 (0.03)	0.59 (0.32)	–	–	–
NGC 3898	0.16 (0.13)	2.71 (0.88)	0.08 (0.08)	1.79 (0.70)	33.0 (20.5)	18.0 (7.0)	360 (50)
NGC 4378	0.78 (0.30)	2.51 (0.48)	0.52 (0.21)	1.55 (0.31)	–	–	–
NGC 4419	0.16 (0.09)	1.27 (0.23)	0.07 (0.05)	0.72 (0.20)	–	–	–
NGC 4450	0.50 (0.06)	1.49 (0.37)	0.34 (0.01)	0.81 (0.18)	28.4 (7.7)	–	–
NGC 4698	0.32 (0.31)	2.76 (0.44)	0.19 (0.19)	2.04 (0.71)	29.5 (17.6)	25.8 (10.0)	339 (50)
NGC 4845	1.90 (0.33)	1.32 (0.19)	0.73 (0.14)	0.77 (0.11)	–	–	–
NGC 5879	0.08 (0.08)	0.89 (0.30)	0.05 (0.05)	0.58 (0.19)	19.1 (0.8)	–	–
NGC 6314	0.83 (0.15)	1.49 (0.40)	0.38 (0.05)	0.98 (0.31)	–	–	–
IC 724	1.63 (0.36)	1.66 (0.26)	0.70 (0.12)	0.94 (0.10)	–	–	–

Notes Columns 2-5: M/L's are in solar units

Table 3. Masses of the components.

Name	M_b	M_d	M_V	M_h	M_{tot}	M_h/M_V
(1)	(2)	(3)	(4)	(5)	(6)	(7)
NGC 1024	17.26 (0.47)	9.74 (1.35)	27.01	–	27.01	–
NGC 2639	0.22 (0.43)	25.98 (2.27)	26.19	16.60 (1.70)	42.79	0.64
NGC 2775	8.62 (1.63)	18.35 (2.76)	26.97	–	26.97	–
NGC 2841	7.13 (0.98)	29.97 (6.07)	37.11	10.60 (0.60)	47.71	0.28
NGC 3593	0.12 (0.08)	2.21 (0.72)	2.33	–	2.33	–
NGC 3898	0.98 (1.03)	17.77 (3.71)	18.74	14.40 (4.70)	33.14	0.77
NGC 4378	5.29 (1.06)	22.60 (1.88)	27.89	–	27.89	–
NGC 4419	0.24 (0.14)	4.91 (0.72)	5.16	–	5.16	–
NGC 4450	1.25 (0.49)	13.05 (2.64)	14.30	10.60 (2.90)	24.90	0.75
NGC 4698	0.84 (0.98)	16.49 (4.18)	17.34	3.70 (1.90)	21.04	0.22
NGC 4845	2.52 (0.62)	7.43 (1.97)	9.95	–	9.95	–
NGC 5879	0.02 (0.02)	1.69 (0.15)	1.71	4.70 (0.20)	6.41	2.78
NGC 6314	9.64 (1.31)	23.84 (3.65)	33.48	–	33.48	–
IC 724	20.86 (5.41)	30.21 (3.22)	51.07	–	51.07	–

Notes. Column 2: bulge mass; *Column 3*: disk mass; *Column 4*: bulge + disk mass;
Column 5: halo mass; *Column 6*: total mass (all values are in units of 10^{10} M$_\odot$).
Column 7: dark–to–visible mass ratio.

The mean colors and M/L's of bulges and disks are plotted in Fig. 3 together with the two SPS models. The average M/L for the bulges are computed excluding values below 0.2 in all bands. W94 colors and M/L's agree rather well with the observed values, whereas BC95 have both bluer colors and lower M/L's. The discrepancies between the two models have been discussed by Charlot et al. (1996). Inspection of the left panel of Fig. 3 shows that bulges are notably redder than disks, both in $r - K$ and in $J - K$ (see also Paper I). Nevertheless, the discrepancies between different SPS models, the degeneracy age/metallicity, and the possible effect of extinction make the color-color plot in Fig. 3 ambiguous as a diagnostic for distinguishing different stellar populations.

Fortunately, M/L ratios disentangle, at least partly, the ambiguity of age and metallicity. We find that bulges, on average, have lower M/L's than disks in all bands[1]. Moreover, the values of M/L seen in the right panel of Fig. 3, according to the SPS predictions, suggest that bulges are *younger* and *more metal rich* than disks. We note that both W94 and BC95 models of a given abundance follow approximately the same trend with age. Hence, the displacement of the bulge and disk values relative to

_____

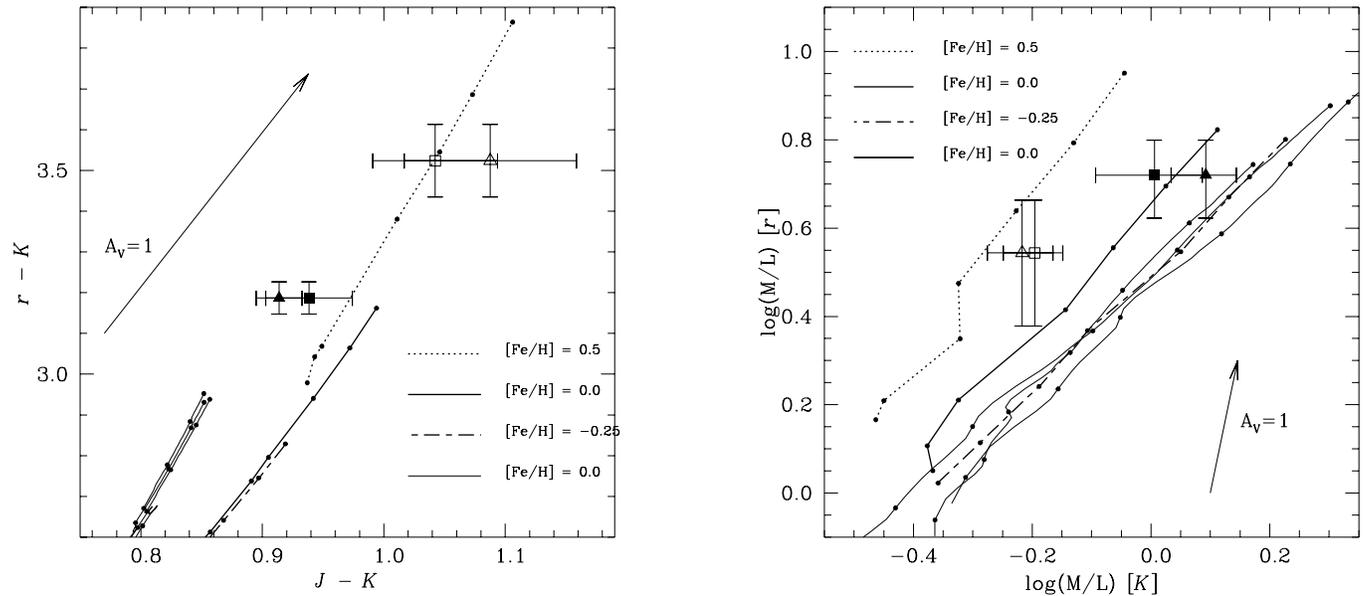[1] J is not shown in the Fig. 3, but J-band M/L's behave in the same way as those in r and K.

Fig. 3. *Left panel:* Comparison of average component colors to models of stellar population synthesis. The three thick lines with marked dots correspond to models (W94) with different metallicities as labelled: [Fe/H]=0.5 [Fe/H]=0.0, and [Fe/H]=-0.25. Age increases from bottom to top; designated points correspond to ages of 1.5, 2, 3, 5, 8, 12, 17 Gyr. The three thin continuous lines correspond to models (BC95) with fixed solar metallicity and different IMF's. Dots mark the same ages as for W94. models. Filled symbols represent the average colors of disks with the relative uncertainties; the triangle is for the parametric results and the square for the non parametric ones. Empty symbols are the bulge values. *Right panel:* the same comparison for M/L's (r and K bands).

that trend implies that bulges are characterized by a younger age than that of the disks, independently of discrepancies between models. Except for extreme inclinations, $i > 75°$, dust in the central regions affects the bulge more than the disk (Bianchi et al. 1996). Consequently, the noted difference between bulge and disk M/L cannot be attributed to internal extinction, since the correction would only increase the difference between the two. The possibility that the disk M/L's have been overestimated seems rather unlikely, even under the MBD hypothesis (although see Bottema 1997; Courteau & Rix 1997) since an average error greater than 30% on the estimated disk RC contribution would be required to make the disks' average age comparable to bulges'. Finally, the bulge M/L's could have been systematically underestimated. This would be the case only if all the RC's (and not just the few already noted and excluded from the mean) rose too slowly in the inner regions with respect to the true circular velocity of the galaxy. We discussed briefly this point in Sect. 3.2, concluding that most likely such underestimates, if present, are not sufficient to eliminate the observed difference in M/L between the components.

That bulges may be more metal rich than disks is not a new result (Bica & Alloin 1987; Delisle & Hardy 1991; Giovanardi & Hunt 1996; Paper I), and abundance variations are thought to be driven by variations with mass (e.g., Zaritsky et al. 1994). That bulges appear to be *younger* than disks is somewhat surprising; the comparison with SPS models shown in Fig. 3 implies an age difference of around 50%, or 5 Gyr. Nevertheless, such a result may be interpreted in light of recent observational and theoretical work on bulge dynamics. Many bulges

show kinematic and photometric signatures usually associated with disks, including flattened distributions, exponential falloff, dominance of the rotation velocity component, and spiral structure in the bulge-dominated region (Kormendy 1993 and references therein). Moreover, some bulges have blue colors, the result of extremely young populations (Schweizer 1990), and as noted in Paper I, at least three of the galaxies in our sample appear to be actively forming stars[2]. As suggested by Kormendy and others, "bulges" may be built up over time from disk material transported to the central regions by gravitational perturbations; such bulges would appear younger than the disks from which they derive.

4.2. Correlations with mass-to-light ratios

Since, as for the photometric properties discussed in Paper I, disk characteristics are more reliably determined than those of bulges, we will concentrate on the M/L's obtained for the disks.

Several authors (see for instance Djorgovski & Santiago 1993, and references therein) have demonstrated that elliptical galaxies follow a relation which can be expressed in terms of a power law: M/L $\propto L^\alpha$ with $\alpha = 0.2 \sim 0.3$ depending on the sample and the photometric band. Kent (1986) also found that the disks of spirals follow a similar relation in the r band at fixed morphological type with an exponent $\alpha = 0.18 \pm 0.07$. More recently Persic, Salucci, and collaborators (PSS; Salucci et al. 1991) found for a sample of late-type spirals that in B,

---

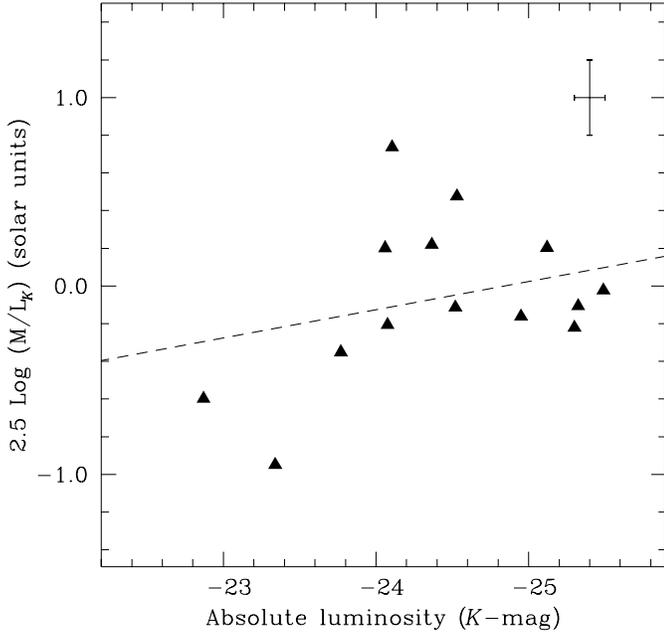[2] Two of these have, however, been excluded from the calculation of the mean.

Fig. 4. The M/L vs luminosity for the disks (K band) with the trend derived from α_B and the color-luminosity relation described in the text.

$\alpha = 0.30 \sim 0.35$. Burstein et al. (1997) have suggested that a relation of this kind between M/L and luminosity is common to all the self-gravitating structures in the universe, ranging from globular clusters to clusters of galaxies. Finally, models of cold dark matter halos, based on N-body simulations and adiabatic infall for disk formation, require a variation of disk M/L with B luminosity in order to accommodate observed rotation curves (Navarro et al. 1996).

We have investigated the compatibility of the values of α found in the optical with our K-band data, assuming the trend of M/L with L is due to disk stars and not to DM. We can convert the index α_B found in the B band to the K-band value using the well-established color–luminosity relation for spirals (Visvanathan 1981; Wyse 1982; Tully et al. 1982). Based on recent data, Gavazzi (1993) finds:

$$B - H = -0.2\,\mathcal{M}_H + const.$$

for early-type spirals. If we assume that $H - K$ is independent of luminosity (which is likely since $H - K$ is typically small, ~ 0.2 mag), then we have a similar relation for $B - K$ with

$$B - K = -0.2\,\mathcal{M}_K + const. \ .$$

We take $\alpha_B = 0.35$ (PSS) together with the slope of the color–luminosity relation defined above, we infer a value of $\alpha_K = 0.15$. If we *fit* our data to a regression of M/L versus disk luminosity, we obtain $\alpha_K = 0.22 \pm 0.15$, consistent with the expected value of 0.15. Fig. 4 shows K-band disk luminosity plotted against disk M/L (K), together with a line having slope $\alpha = 0.15$.

The M/L vs luminosity relation for elliptical galaxies is implicit in a more general relation, namely the one defining the

fundamental plane (FP) of elliptical galaxies (see review by Kormendy & Djorgovski 1989):

$$R_e \propto \sigma_c^a I_e^b \qquad (12)$$

where R_e and I_e are respectively the effective radius and surface brightness and σ_c is the observed central velocity dispersion[3]. We have fitted a similar relation between disk scale lengths, central brightnesses, and peak rotation velocities of our disks, and find: $a = 1.2 \pm 0.2$ and $b = -0.84 \pm 0.1$. This implies that the disks of early-type spirals also define a plane similar to that for ellipticals; the elliptical FP has $a = 1.4 \pm 0.15$ and $b = -0.9 \pm 0.1$. A similar result, but for the photometric properties only, was reported in Paper I, both for bulges and disks. When we derive the M/L vs L relation from Eq. 12 and the virial theorem we obtain:

$$M/L \propto L^{\frac{2-a}{2a}} I(0)^{-\frac{a+4b+2}{2a}}$$

which contains a residual dependence on the central brightness $I(0)$. However our values for a and b yield

$$M/L \propto L^{0.3} I(0)^{-0.07}$$

where, as for ellipticals, the dominant dependence is on luminosity.

As discussed by Djorgovski & Santiago (1993), a relation between M/L and luminosity (or mass) can come about in several ways. One possibility is that the disk M/L's are contaminated by a DM contribution which has a density profile similar to that of the stellar disk. The sense of the M/L vs L relation would require this DM fraction to increase with luminosity, contrary to the trend observed for the global DM fraction which increases with *decreasing* luminosity (e.g., PSS). Alternatively, the MBD hypothesis could be incorrect, and the stellar disk M/L constant. In this case, though, the trend in Fig. 4 would require the MBD hypothesis to be more valid in lower luminosity systems, contrary to common beliefs.

Another possibility is that disks of different luminosities harbor different stellar populations, which is also suggested by the color-luminosity relation mentioned above. W94 predicts that at fixed age, initial mass function (IMF), and star formation rate (SFR), M/L is an increasing function of metallicity in the optical, but a *decreasing* one in the NIR. This suggests that the M/L vs L correlation cannot be understood in terms of a metallicity variation. Alternatively, such a correlation could be driven by a change of average age or star formation history with luminosity. Again, the observed difference in the slope of the correlation at different wavelengths can be compared to the predictions of SPS models. To test this possibility we made use of the BC95 models, at fixed (solar) metallicity and IMF (Salpeter 1955), considering single burst populations at different age T, and populations

---

[3] We note that for elliptical galaxies the central observed velocity dispersion depends on *total* mass, whereas RC fitting in principle disentangles the contributions of stars and DM. If we assume, following Salucci & Persic 1997, that the fractional DM content is a decreasing function of luminosity also for ellipticals, an M/L vs L relation for the stellar component alone would require a steeper slope than the one derived from the FP relation.

with different e-folding time τ (exponential SFR) at fixed age (10 Gyr). We have approximated the model dependence of M/L on T and τ with power laws, whose index in B and K has been determined with a best fit. Assuming $M/L_B \propto L^{0.35}$, in the first case the model predicts a difference in the slope of this relation of 0.17 passing to the K band, consistent with the predicted difference of ~ 0.2. Considering the variation with τ the prediction is ~ 0.2, in similarly good agreement. It, therefore, seems plausible that the variation of M/L with luminosity is driven by different star formation histories, and the consequent different stellar mixes.

4.3. Dark halos

We claim to recognize the presence of a dark halo in six of our galaxies: three of them are pseudo-isothermal and three constant-density spheres. We do not find any systematic difference between the two models, at least in terms of central densities or masses within R_{25}. The statistics are sparse, but we can attempt a comparison with the general relations found by PSS in the B band for a large sample of late-type spirals. In particular, we can check that the ratios of the halo central density to the critical density, ρ_0/ρ_c, and the dark to visible mass at the optical radius, M_h/M_V, are consistent with the correlations with the B-band galaxy luminosity given in PSS. They find:

$$\frac{M_h}{M_V} = 0.4 \left(\frac{L_B}{L_B^*}\right)^{-0.9} \quad \text{and} \quad \frac{\rho_0}{\rho_c} = 3.5 \cdot 10^4 \left(\frac{L_B}{L_B^*}\right)^{-0.07}$$

with $L_B^* = 10^{10.4} L_B^\odot$. If we assume the same color–luminosity relation as in Sect. 4.2, we find in the K band after scaling to $H_0 = 50 \, \mathrm{km \, s^{-1}}$:

$$\frac{M_h}{M_V} = 0.8 \left(\frac{L_K}{L_K^*}\right)^{-0.7} \quad \text{and} \quad \frac{\rho_0}{\rho_c} = 3.7 \cdot 10^4 \left(\frac{L_K}{L_K^*}\right)^{-0.06} \quad .$$

with $\rho_c = 3H_0^2/8\pi G = 0.5 \cdot 10^{-29} \, \mathrm{g \, cm^{-3}}$ and $\mathcal{M}_K^* = -23.97$, the absolute magnitude corresponding to L_K^*. We estimated $\mathcal{M}_K^*$ from the color–luminosity relation, with the zero order coefficient fixed by the median values of $\mathcal{M}_B$ and $B-K$ for our sample.

The trends shown in Fig. 5 are consistent with the anticorrelation between dark and luminous mass found in PSS. Moreover, there is no striking discrepancy between our galaxies and the behavior of later type systems, suggesting that dark halos are similar for all spirals. In the right panel of Fig. 5 our data reveal roughly the same M_h as found in late-type galaxies with the same B luminosity.

5. Summary

We summarize here the main conclusions of this paper.

1) The comparison of bulge and disk NIR average colors and mass-to-light ratios to stellar population synthesis models suggests that the bulges of our sample galaxies are younger and more metal rich than the disks.

2) NIR M/L's appear to vary with disk luminosity, consistently with the trend in the B band, and the $B-K$ color–luminosity relation. Such a trend can be probably imputed to a systematic variation of the disk average stellar population with luminosity, due to a variation of either star formation history or age, but not of metallicity.

3) We find no clear evidence to prefer either standard Newtonian gravitation plus dark halos or modified gravitation, as the quality of the fits under both paradigms is comparable. The value of the critical acceleration parameter a_0 that best accommodates the sample as a whole is $1.3 \cdot 10^{-8} \, \mathrm{cm \, s^{-2}}$.

4) The dark halo parameters we obtain for six of our galaxies are roughly in agreement with the values obtained for late type spirals from B-band photometry. In particular our data are consistent with the correlation, already noted by PSS, between dark-to-visible mass ratio and luminosity.

Appendix A: The strip brightness method to derive the luminosity density of an axisymmetric ellipsoid

The strip density method was first introduced by Schwarzschild (1954) to evaluate the gravitational potential of the Coma cluster. In the following we describe the method and extend it to the more general situation of an oblate, axisymmetric, ellipsoidal distribution of mass (and luminosity). This technique offers a quite simple and straightforward way to recover the spatial density distribution, and the potential and rotation curve of such systems, especially when they are not described parametrically but rather observed as projected distributions on the sky.

Let us consider an ellipsoidal distribution, centered at O, with oblate rotational symmetry about z, inclined by an angle i to the line of sight [Fig. 6(b)]. The isodensity surfaces can be parametrized by their semimajor axis, that is their equatorial radius a:

$$j(x, y, z) = j(a) \; ,$$
$$\text{with } a = \sqrt{x^2 + y^2 + \frac{z^2}{1 - \epsilon^2}} \quad , \tag{A1}$$

where the constant $\epsilon = \sqrt{1 - \frac{b^2}{a^2}}$ is the intrinsic eccentricity. The projected distribution on the plane of the sky (ξ, η) has elliptical symmetry with an apparent eccentricity $\epsilon \sin i$. The surface brightness is then

$$I(\xi, \eta) = I(q) \; ,$$
$$\text{with } q = \sqrt{\xi^2 + \frac{\eta^2}{1 - (\epsilon \sin i)^2}} \quad . \tag{A2}$$

We now define the strip brightness at distance ξ_0 from the image minor axis [Fig. 6(a)] as

$$S(\xi_0) = \int_{-\infty}^{+\infty} I(\xi_0, \eta) \, d\eta \; . \tag{A3}$$
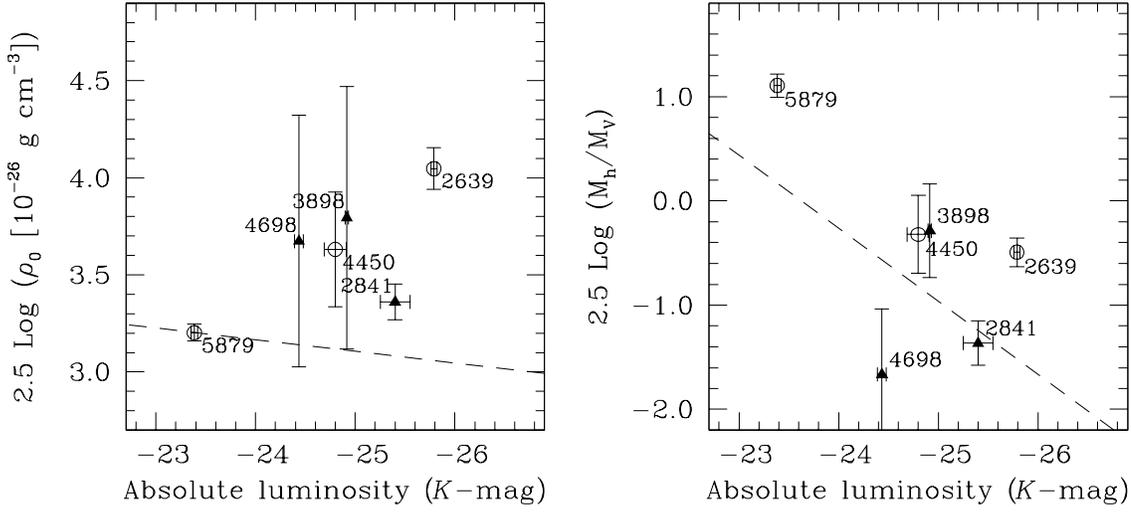
Fig. 5. Central halo density and ratio of dark to visible mass vs galaxy K absolute magnitude. Filled triangles correspond to isothermal halos, open circles to constant density ones. The dashed lines represent the NIR relations between these parameters corresponding to the ones obtained by PSS in the B band.
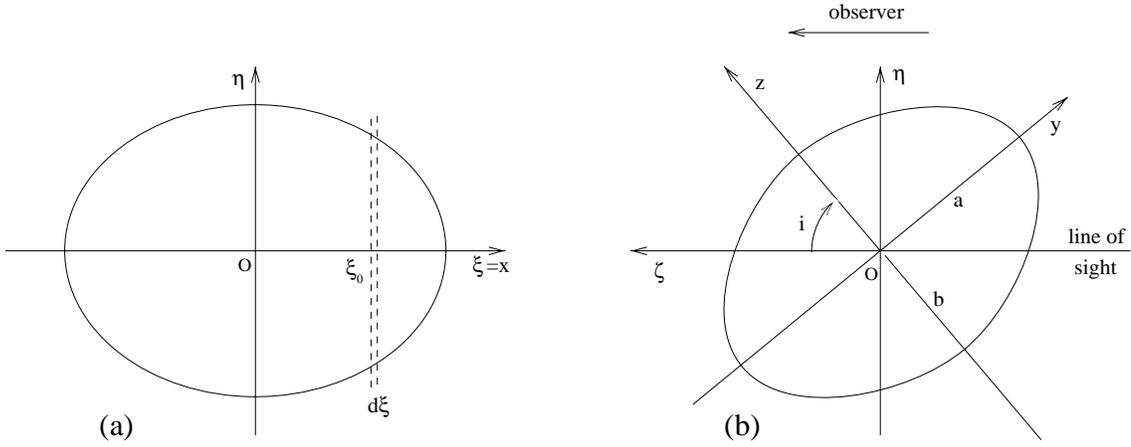

Fig. 6a and b. Geometry of the ellipsoid **a** as seen projected on the sky plane, and **b** from a lateral viewpoint. The symmetry axis z is inclined with respect to the line of sight and the axes x and ξ coincide with the line of nodes, interception of the equatorial plane (x, y) with the sky plane (ξ, η). The *strip brightness* is the integral of the surface brightness along a strip perpendicular to the line of nodes, as sketched by the dashed lines in panel **a**.

On the other hand $S(\xi_0)$ is the luminosity of a section perpendicular to x at $x = \xi_0$ of the ellipsoid. Such a section will have again elliptical symmetry with eccentricity ϵ. Any elliptical isodensity contour of this section can be described by:

$$y^2 + \frac{z^2}{1 - \epsilon^2} = a^2 - \xi_0^2 \ ,$$

and area $A(a, \xi_0) = \pi \sqrt{1 - \epsilon^2} \, (a^2 - \xi_0^2) \ .$ (A4)

Then,

$$S(\xi_0) = \iint j(x = \xi_0, y, z) \, dy \, dz$$

$$= \int j(a) \, dA = 2\pi \sqrt{1 - \epsilon^2} \int_{\xi_0}^{\infty} j(a) \, a \, da$$ (A5)

and

$$\frac{dS}{d\xi_0} = -2\pi \sqrt{1 - \epsilon^2} \, \xi_0 \, j(a = \xi_0)$$ (A6)

In practice, the observed image is divided in strips normal to ξ and integrated in the η direction. This gives $S(\xi_0)$ for ξ_0 spanning from 0 to the outermost radius of the image. Eq. A6 is then used to derive $j(a)$, and with it the potential and circular speed. From a numerical point of view the method is easy to implement and was tested on a number of analytical solutions. Due to the strip integration prior to the differentiation in Eq. A6, the noise introduced is low and hardly appreciable even in the outer regions.

References

Begeman K.G. 1987, Ph.D. Thesis

Begeman K.G., Broeils A.H., Sanders R.H. 1991, MNRAS 249, 523

Bertola F., Cinzano P., Corsini E.M., et al. 1996, ApJ 458, L67

Bianchi S., Ferrara A., Giovanardi C. 1996, ApJ 465, 127

Bica E., Alloin D. 1987, A&AS 70, 281

Binney J., Tremaine S. 1987, Galactic Dynamics, Princeton University Press (Princeton, New Jersey)

Bottema R. 1997, A&A 328, 517

Broeils A.H. 1992, Ph.D. Thesis, University of Groningen

Broeils A.H., Van Woerden H. 1994, A&AS 107, 129

Bruzual G., Charlot S. 1993, ApJ 405, 538

Burstein D., Bender R., Faber S.M., Nolthenius R. 1997, AJ 114, 1365

Charlot S., Worthey G., Bressan A. 1996, ApJ 457, 625

Courteau S., Rix H.-W. 1997, ApJL, submitted (astro-ph/9707290)

Delisle S., Hardy E. 1991, AJ 103, 711

Demoulin M.H. 1969, ApJ 157, 75

de Vaucouleurs G., de Vaucouleurs A., Corwin H.G., Buta R.J., Paturel G., Fouqué P. 1991, Third Reference Catalog of Bright Galaxies, Springer Verlag (New York) (RC3)

Djorgovski S., Santiago B.X. 1993, in Structure, Dynamics and Chemical Evolution of early-type Galaxies, eds. Danziger et al.

Fillmore J.A., Boroson T.A., Dressler A. 1986, ApJ 302, 208

Freeman K.C. 1970, ApJ 160, 811

Gavazzi G. 1993, ApJ 419, 469

Giovanardi C., Hunt L.K. 1996, AJ 111, 1086

Guhathakurta P., Van Gorkom J.H., Kotanyi C.G., Balkowski C. 1988, AJ 96, 851

Kent S.M. 1986, AJ 91, 1301

Kent S.M. 1987, AJ 93, 816

Kent S.M. 1988, AJ 96, 514

Kormendy J. 1990 in The Evolution of the Universe of Galaxies, ed. R. Kron (ASP Conf. Ser., 10), 33

Kormendy J. 1993 in Galactic Bulges, ed. H. Dejonghe, H.J. Habing, IAU Symp. 153 (Kluwer, Dordrecht), p. 209

Kormendy J., Djorgovski S. 1989, Ann. Rev. of Astr. & Ap., 27, p. 235

Krumm N., Salpeter E.E. 1979, ApJ 228, 64

Milgrom M. 1983, ApJ 270, 365

Moriondo G., Giovanardi C., Hunt L.K. 1998, A&AS, 130, 81 (Paper I)

Navarro J.F., Frenk C.S., White S.D.M. 1996, ApJ 462, 563

Persic M., Salucci P., Stel F. 1996, MNRAS 281, 27

Rubin V.C., Burstein D., Kent Ford Jr W., Thonnard N. 1985, ApJ 289, 81

Salpeter E.E. 1955, ApJ 121, 61

Salucci P., Persic M. 1997, in Dark & visible Matter in Galaxies, ed. Persic, M., Salucci, P.

Salucci P., Ashman K.M., Persic M. 1991, ApJ 379, 89

Sanders R.H. 1990, A&AR 2, 1

Schwarzschild M. 1954, AJ 59, 273

Schweizer F. 1990, in Dynamics and Interactions of Galaxies, ed. R. Wilen (Springer-Verlag, Berlin), p. 60

Toomre A. 1963, ApJ 138, 385

Tully R.B., Mould J.R., Aaronson M. 1981, ApJ 257, 527

Van Driel W., Van Woerden H. 1991, A&A 243, 71

Visvanathan N. 1981, A&A 100, L20

Van Albada T.S., Sancisi R. 1986, Royal Society Discussion on Material Content of the Universe, Philosophical Transactions, Series A, N. 1556, 447

Warmels R.H. 1986, in HI Properties of Spiral Galaxies in the Virgo Cluster, University of Groningen

Worthey G. 1994, ApJS 95, 107

Wyse R.F.G. 1982, MNRAS 199, 1P

Zaritsky D., Kennicutt R.C. Jr., Huchra J.P. 1994, ApJ 420, 87